

Reaction mechanisms of low-kinetic energy hydrocarbon radicals on typical hydrogenated amorphous carbon (a-C:H) sites: A molecular dynamics study

E. Neyts^{*}, M. Tacq, A. Bogaerts

University of Antwerp, Department of Chemistry, PLASMANT research group, Universiteitsplein 1, B-2610 Antwerp, Belgium

Received 24 August 2005; received in revised form 8 February 2006; accepted 15 February 2006

Available online 6 March 2006

Abstract

In this work, we have investigated reaction mechanisms of several hydrocarbon radicals on specific sites, relevant for a-C:H thin films. This study has been carried out using classical molecular dynamics simulations. The species whose reaction mechanisms have been studied, include C₂, C₃, linear C₃H and cyclic C₃H. In total, 9 surface sites have been investigated. Several trends in the mechanisms have been established. It is shown that chemical resonance, steric hindrance and structural stability are the main factors affecting the reaction mechanisms. Also, the influence of site-specific factors is addressed. This information is important for a better understanding of the growth of thin a-C:H films from low-kinetic energy hydrocarbons.

© 2006 Elsevier B.V. All rights reserved.

Keywords: a-C:H; Hydrocarbon reaction mechanisms; Molecular dynamics

1. Introduction

Thin a-C(:H) films have attracted much attention since their first preparation in the early 70s [1], both by experimental and computational means. It is well known that several types can be distinguished. The hardest materials, often called tetrahedral amorphous carbons, or ta-C, are characterised by a high hardness and Young's modulus, a low roughness and a very low friction coefficient [2,3]. When hydrogen is incorporated into this type of film, tetrahedral hydrogenated amorphous carbon, of ta-C:H is obtained. Experimentally, these materials are most often fabricated using an ion-source, producing high-energy carbon or hydrocarbon ions (~100 eV) bombarding the substrate. The high-energy ions can penetrate into the sub-surface layers, causing a local increase in the density. The local bonding will then reform according to this new density, leading to a high sp³ fraction.

The most widely used hard carbon coatings, however, are the so-called 'diamond-like carbons', or DLCs, with hardness values of up to 20 GPa [4,5]. These films are often produced by plasma processes, such as plasma enhanced chemical vapor deposition

(PECVD). In contrast to the deposition of ta-C(:H), the ion flux fraction is now much lower than 100%, the exact value depending on the type of source used. If high energy ions are present, they can still contribute to the film growth by the same mechanism as for ta-C. However, in this case, also neutral species will contribute to the growth. Whether the subplantation mechanism will be operative under these conditions depends on the ion/radical flux ratio and the ion energy. In contrast to ta-C(:H), DLCs do not possess a predominant tetrahedral structure.

These classes of hard films (ta-C(:H) and DLC) are used for example as wear-resistant coatings, on, e.g. magnetic hard disks and optical components.

The softer type of materials, which can be referred to as (hydrogenated) amorphous carbon, of a-C(:H), can still exhibit a considerable hardness, good adhesion and chemical stability [4,6], and can be used as, e.g. solid lubricants. This type of films can also be produced by, e.g. PECVD [2]. The contribution of the neutral species will depend on their individual sticking coefficients. Diradicals can insert directly into surface C–C or C–H bonds, such that their sticking coefficient approaches 1. Monoradicals cannot insert directly into surface bonds, but need a dangling bond at the surface. This dangling bond can be created by removal of a hydrogen atom from a C–H surface bond, either by ion displacement of H, or by H-abstraction [7].

^{*} Corresponding author.

E-mail address: erik.neyts@ua.ac.be (E. Neyts).

Closed shell neutrals show sticking coefficients close to zero, and their effect on the growth is negligible. In contrast to the subplantation mechanism in ta-C(:H) growth, which is a physical process, the deposition mechanism of a-C(:H) films occurs through a combination of physical subplantation and chemical surface reactions if ions are present, or entirely through chemical reactions if no ions are present. In the simulations presented in this work, we have studied chemical surface reactions involving radicals only, without concurrent ion bombardment.

It is clear that a good understanding of the reaction mechanisms of the hydrocarbon radicals at the surface is of paramount importance. In general, the identity of the exact growth precursors is often unknown. Therefore, a good understanding of the growth process can only be obtained quantifying all relevant contributions. In the present work, however, we have chosen to investigate the behaviour of several hydrocarbon radicals of which it is known that they are important for the growth of a-C:H films using the expanding thermal plasma source (ETP) [8]. These species are C_2 , C_3 , linear C_3H (*l*- C_3H) and cyclic C_3H (*c*- C_3H). The paper is organized as follows: the simulation model and the sites on which the impacts are performed are described in Section 2. The reactions and their mechanisms are discussed in Section 3, and finally, a conclusion will be given in Section 4.

2. Description of the simulations

The model used for this investigation, is a classical molecular dynamics model. The model was originally developed by Serikov et al. [9], and subsequently modified. The interatomic potential used is the well-known Brenner potential for hydrocarbons [10]. In this methodology, the atoms in the system are followed through space and time by integrating Newton laws. The atoms move under the influence of forces, taken as the negative of the analytical derivative of the interatomic potential. The integration scheme used is the velocity–Verlet algorithm [11]. The time step used is 0.2 fs.

To investigate the reaction mechanisms, several surfaces are created containing specific sites on which the impact of the hydrocarbon radicals will be performed. The surface itself is either a non-passivated, non-reconstructed diamond {111} surface, or a H-passivated non-reconstructed diamond {111} surface. A site is defined as a specific location on this surface: it can be a dangling bond, or one or several atoms bound on top of the diamond surface, corresponding to sites as they are grown during, e.g. a deposition process. The main difference between a diamond substrate containing specific a-C:H sites (as used in this work), and a ‘true’ a-C:H surface, is the bond angle and bond length distribution, possibly influencing the site-specific system reactivity. Therefore, the current model system was chosen in order to obtain a well defined system.

The first site investigated is simply one of the 3-coordinated carbon atoms on the non-passivated diamond surface, i.e., with a dangling bond. All other sites were created starting from the passivated surface. On two of the 9 sites, two different locations have been selected, such that in total 11 site locations were

investigated (sites O7/O8 and O10/O11 in Fig. 1). All 11 sites simulated in this work are depicted schematically in Fig. 1.

Initially, the substrate is relaxed at 100 K using the Berendsen heat bath algorithm [12]. The hydrocarbon radical is positioned at a specified $\{x, y\}$ position above the site of interest at a z -position beyond the cut-off of the potential. The orientational angles of the hydrocarbon radical are chosen at random. The atoms in the substrate are allowed to move freely according to the forces acting upon them, except for the site-atoms. These are kept fixed, until the potential energy between one of the site-atoms and the hydrocarbon radical becomes negative, in order to make sure that the radical impinges exactly on the required position on the site. During the impact, no heat bath is applied. The hydrocarbons were given a kinetic energy of 0.13 eV (translational motion in the z -direction), corresponding to the experimentally determined gas temperature of about 1500 K [8], and a vibrational energy of 0.026 eV.

Each impact of a specified hydrocarbon radical on a specific site location is repeated 100 times. Although this gives rather poor statistics on rarely occurring reactions, it is sufficient to determine the major reaction mechanisms, which is the goal of this study. In total, 4400 impacts have been performed and analysed.

In Table 1, the different hydrocarbon radicals investigated in this work are shown with their major resonance contributors. In Table 2, these species are shown with their gas-phase binding energies, as calculated using the Brenner potential.

3. Results and discussion of the reaction mechanisms

3.1. Sites O1, O2 and O3

Site O1 is a 3-coordinated carbon atom, i.e., a dangling bond, on the non-passivated diamond surface. Site O2 is a dangling bond on the passivated diamond surface, created by H-abstraction from this surface. Site O3 is a H-atom on the passivated, non-reconstructed diamond {111} surface. Note that all species investigated are reflected for 100% on site O3. The results for sites O1 and O2 are summarised in Table 3.

3.1.1. Impact of C_2

The C_2 radicals show a sticking coefficient of 100% on sites O1 and O2. This is caused by the fact that C_2 is small (no steric hindrance), and both the carbon atoms of the C_2 radical, as well as the surface carbon atom, have a free electron to participate in the binding. The binding energy between the surface carbon (from here on denoted as “ C_s ”) and the binding radical atom is calculated to be -3.57 eV, both for O1 and O2. Note that the average single C–C bond strength is about -3.60 eV, a double bond about -6.36 eV and a triple bond about -8.70 eV.

The intramolecular C–C bond of the radical becomes stronger upon sticking by more than 28% on both sites, to a value of -7.67 eV. Hence, there is a shift from the sp^2 resonance contributor (having a double bond) in the gas phase to the sp resonance contributor (having a triple bond) after sticking to the surface (see Fig. 2). An example of the evolution of the binding energy as a function of time is shown in Fig. 3 for the O1 site.

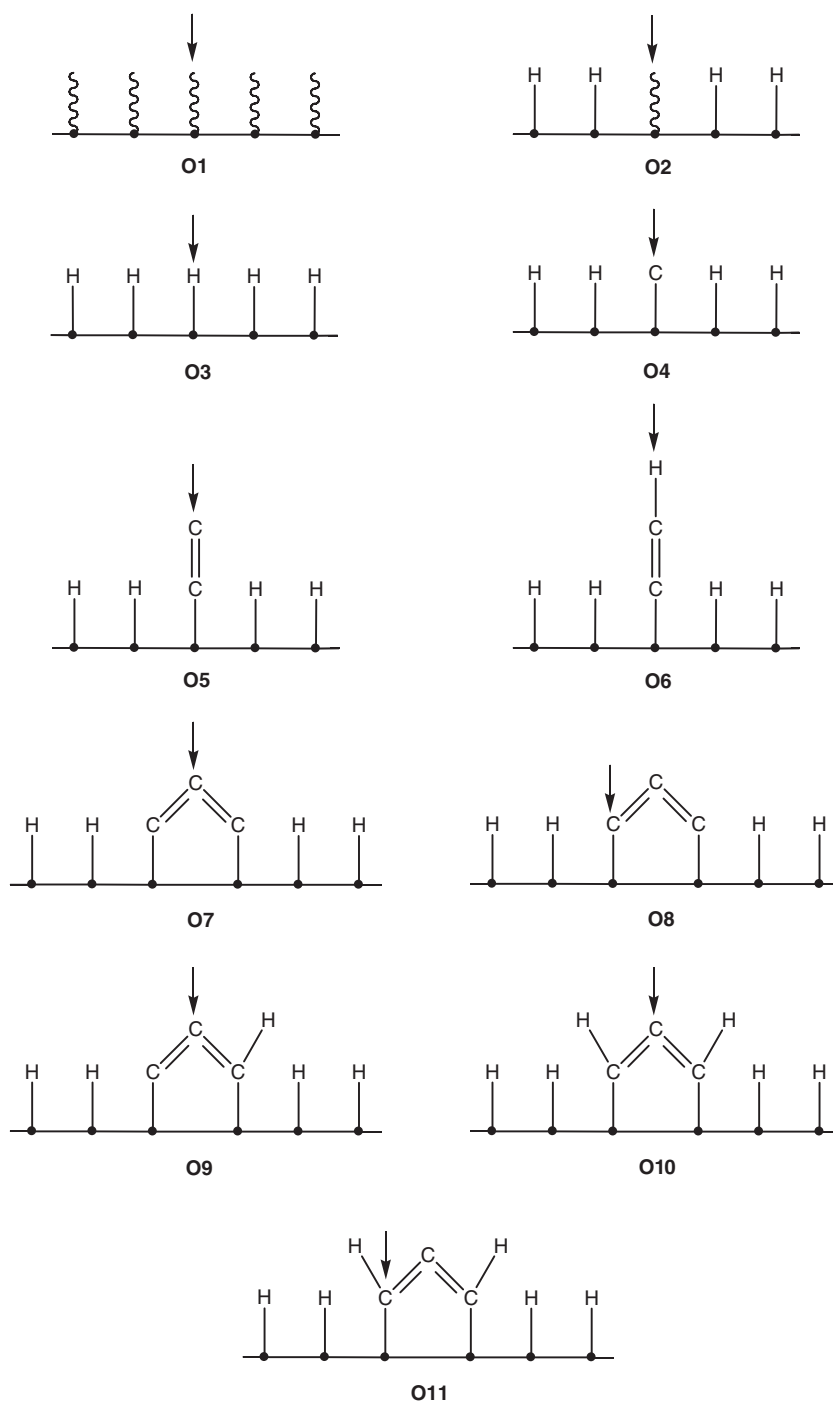


Fig. 1. Schematic representation of the sites studied in this work. The 11 impact locations are denoted as O1 to O11. Locations O7 and O8, and O10 and O11 share the same site, but the impact position of the hydrocarbon radical on the site is different. The exact impact location is indicated by the arrows. The dots in the figure indicate surface carbon atoms, and the wavy lines symbolize a dangling bond.

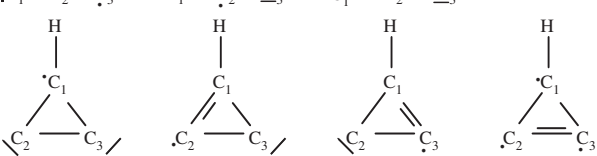
All species are reflected for 100% on site3 as mentioned above. However, in contrast to the other species, the C_2 radical causes the abstraction of the H-atoms in 56% of its impacts, creating a dangling bond. Indeed, while the other species feel no ‘advantage’ in abstracting the H from the surface, the double bond in the C_2 radical becomes a triple bond in this process, in order to accommodate the extra electron, which explains why C_2 is so effective in H-abstraction. This result also suggests that

C_2 radicals can make an a-C:H surface much more reactive, by abstraction of H from a H-passivated surface.

3.1.2. Impact of C_3

In contrast to the C_2 radical, the C_3 radical can bind to the surface in various ways on the O1 site. Only 1% of the impacts on this site resulted in a reflection event. In 73% of the impacts, the C_3 radical binds to the surface with the formation of a single

Table 1
Main resonance contributors for the species investigated

Species	Main resonance contributors
C ₂	$ C=C $ $\cdot C\equiv C\cdot$
C ₃	$ C=C=C $ $\cdot C\equiv C-C\dot{C}$ $\dot{C}-C\equiv C\cdot$
<i>l</i> -C ₃ H	$ C_1=C_2=C_3 $ $ C_1=C_2-C_3 $ $\cdot C_1\equiv C_2-C_3$
<i>c</i> -C ₃ H	

bond, and in the majority of these cases, this occurs with one of the terminating C₃ carbon atoms (61% vs. 12% with the middle carbon atom).

In the remaining 26% of the impacts, the radical binds to the surface with the formation of two bonds, either involving only the terminating carbon atoms (22%), or both with the middle carbon and one of the terminating carbon atoms (4%). Note that in 21% of the impacts, sticking occurs with the formation of a ‘bridge’ structure.

On the O2 site, however, 23% of the impacts leads to reflection, and the only occurring sticking mechanism (77%) is the binding of one of the outer carbon atoms with the surface. In this mechanism, the bond between the surface binding C₃ atom and the middle C₃ atom becomes slightly stronger (about + 1.6%), while the bond between the other outer C₃ carbon atom and the middle C₃ atom becomes slightly weaker (about – 1.0%), both on site O1 and O2. This result is a trend observed throughout all simulations presented in this work.

The reason for the much higher reflection coefficient of C₃ on the O2 site is steric hindrance: the presence of the H-atoms on the O2 site, allows the C₃ radical to stick on this site only vertically, and only with the formation of a bond between the surface atom with the dangling bond, as opposed to the several possibilities on the O1 site.

3.1.3. Impact of *l*-C₃H

The impact of *l*-C₃H on O1 and O2 is comparable to the behaviour of C₃. Similar to C₃, *l*-C₃H shows a very low reflection coefficient of 3% on site O1. In 32% of its impacts on O1, the *l*-C₃H radical binds to the surface with its outer (non-hydrogen carrying) carbon atom, forming a single bond. This is about half compared to the same sticking event of C₃ on site O1. Also, a larger fraction of the sticking events occurs through the middle carbon atom in *l*-C₃H as compared to C₃ (23% of its impacts compared to 12% for C₃). In 28% of the events, a bridge structure is formed between the surface and the two outer carbon atoms of the *l*-C₃H radical.

The formation of the bridge structures can be explained by the resonance contributors (Fig. 4): while in the case of C₃ the C–C bond between the middle carbon atom and the surface binding atom becomes sp-hybridised (triple bond, linear structure), this bond essentially remains a double bond in the

case of *l*-C₃H (sp² hybridised, 120° angle). Hence, the other outer carbon atom remains physically close to the substrate atoms (carrying dangling bonds), and has a free electron left. This then promotes the formation of bridge structures, with almost equal occurrence as the single bond mechanism (i.e., 28% vs. 32%). Note that in Fig. 4, all three resonance contributors are shown. The main contributor, however, is the structure in which both the outer carbon atoms are sp² hybridised.

On the O2 site, the reflection coefficient of *l*-C₃H is calculated to be 49%. Again, this is attributed to the same steric hindrance causing the reflection of C₃ on this site. Since the determining factor in this hindrance is the size of the impinging radical, the reflection should be larger than for C₃, as is indeed calculated. When the *l*-C₃H radicals are not reflected, they stick to the surface mostly with the outer, non-H-carrying C-atom, as is clear from Table 3.

3.1.4. Impact of *c*-C₃H

The *c*-C₃H radical is much more reactive than the linear C₃H radical. It has a sticking coefficient of 1.0 on the O1 site, and of 0.82 on the O2 site. There are two factors responsible for this behaviour. First, it should be noted that the cyclic isomer is structurally unstable. In, e.g. cyclopropane (cyclic C₃H₆), the C–C bonds are about 32% weaker than in the linear propane molecule, due to a severe ring strain of 117 kJ/mol. In *c*-C₃H, the effect is even more pronounced: the C–C bonds in *c*-C₃H are about 50% weaker than in *l*-C₃H. Hence, the release of this ring strain is a driving force for the radical to break up, enhancing drastically its reactivity. The second reason is the fact that in the *c*-C₃H radical, all three C-atoms bear electrons not participating in a bond, while in *l*-C₃H, the middle C-atom is fully bound. Hence, all three C-atoms in the *c*-C₃H radical can bind to the surface, while the middle C-atom in *l*-C₃H experiences repulsive forces from the surface upon impact [13].

Moreover, due to the fact that the *c*-C₃H radical breaks up easily, more binding configurations result. This break-up occurs in 76% of the sticking events on site O1, and in 72% on site O2 (or 59% of the impacts).

The breaking up can occur in several distinct ways. These mechanisms appear on all sites. Of course, the main effect of a break-up event, is the transformation of the cyclic structure in a linear structure. The remaining bonds are strengthened,

Table 2
The investigated species and their binding energies

Species	C–C bond	Binding energy (eV)
C ₂	C–C	–5.976
C ₃	C–C	–5.995
<i>l</i> -C ₃ H	C ₁ –C ₂	–5.993
	C ₂ –C ₃	–6.173
<i>c</i> -C ₃ H	C ₁ –C ₂ , C ₁ –C ₃	–2.805
	C ₂ –C ₃	–3.105

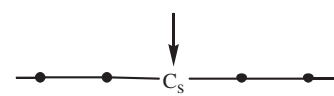
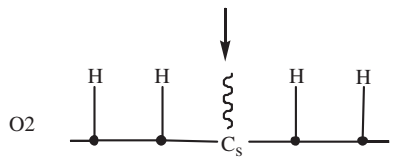

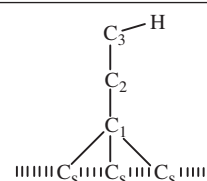
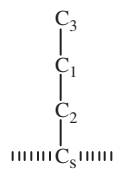
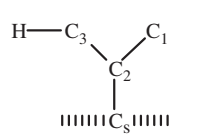
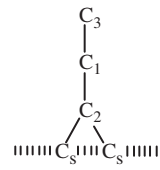
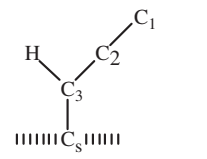
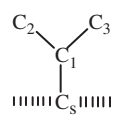
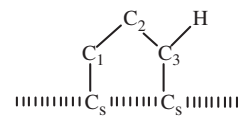
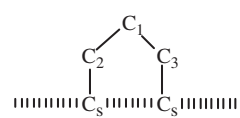
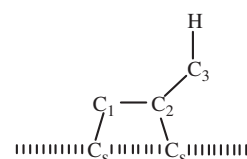
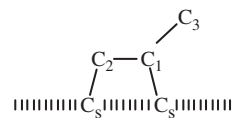
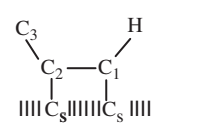
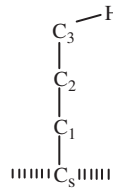
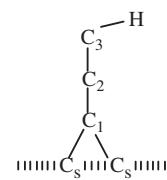
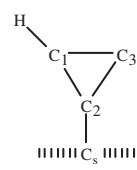
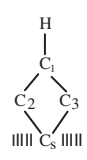
The carbon atom to which the H-atom of the radical is bound, is denoted as C₃ in the *l*-C₃H radical and as C₁ in the *c*-C₃H radical. Note that the binding energy of a single, double and triple C–C bond typically corresponds to –3.60, –6.36 and –8.70 eV, respectively.

depending on which bond is broken and which atom sticks to the surface. As an example, the break-up of a *c*-C₃H radical resulting in a 3-coordinated surface binding atom is shown in

Fig. 5. It is clear from Table 3 that this mechanism, illustrated in Fig. 5, is the most important sticking event of *c*-C₃H on the O1 site and especially on the O2 site.

Table 3

Calculated sticking and reflection coefficients, and sticking structures on sites O1 and O2

Radical	Reflection	Sticking-structures	Sticking	Radical	Reflection	Sticking-structures	Sticking		
									
C ₂	O1 : 0.0 O2 : 0.0		O1 : 1.0 O2 : 1.0	<i>l</i> -C ₃ H continued			O1 : 0.02 O2 : 0.0		
C—C									
C ₃	O1 : 0.01 O2 : 0.23		O1 : 0.61 O2 : 0.77				O1 : 0.23 O2 : 0.03		
C ₂ —C ₁ —C ₃									
			O1 : 0.05 O2 : 0.0				O1 : 0.03 O2 : 0.0		
			O1 : 0.12 O2 : 0.0				O1 : 0.28 O2 : 0.0		
			O1 : 0.17 O2 : 0.0				O1 : 0.06 O2 : 0.0		
			O1 : 0.04 O2 : 0.0				O1 : 0.01 O2 : 0.0		
<i>l</i> -C ₃ H	O1 : 0.03 O2 : 0.49		O1 : 0.32 O2 : 0.48				O1 : 0.02 O2 : 0.0		
<i>c</i> -C ₃ H	O1 : 0.0 O2 : 0.18		O1 : 0.22 O2 : 0.23	<i>c</i> -C ₃ H continued			O1 : 0.04 O2 : 0.0		

(continued on next page)

Table 3 (continued)

Radical	Reflection	Sticking-structures	Sticking	Radical	Reflection	Sticking-structures	Sticking
			O1 : 0.24 O2 : 0.46				O1 : 0.03 O2 : 0.0
			O1 : 0.19 O2 : 0.05				O1 : 0.03 O2 : 0.0
			O1 : 0.09 O2 : 0.04				O1 : 0.03 O2 : 0.0
			O1 : 0.04 O2 : 0.04				O1 : 0.02 O2 : 0.0
			O1 : 0.07 O2 : 0.0				

3.2. Sites O4 and O5

In most cases, the sticking behaviour of the various radicals is very similar on both O4 and O5 sites. In general, the sticking coefficient on site O5 is slightly higher than on O4, due to steric hindrance on site O4, caused by the H-atoms surrounding the site. The results are summarised in Table 4.

3.2.1. Impact of C_2

As already indicated above, the C_2 radical is very reactive. On the O4 site it shows a sticking coefficient of 0.95, and a sticking coefficient of 1.0 on site O5. In most cases, the C_2 radical sticks on site O4 with one of its atoms, but in a few cases, the C–C bond breaks, and both of the atoms bind to the

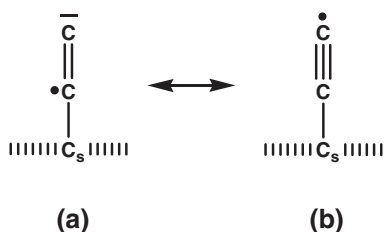


Fig. 2. Resonance contributors for the C_2 radical after sticking to the surface. The sp^2 resonance contributor (a) shifts towards the sp contributor (b) after sticking.

same surface atom. This mechanism does not occur on the O5 site, as appears from Table 4.

3.2.2. Impact of C_3

The sticking coefficient of C_3 is calculated to be very high on the O5 site (0.91), and it is considerably less on the O4 site (0.77). This is entirely due to steric hindrance by the surrounding H-atoms on the O4 site. This radical invariably sticks with one of its outer C-atoms and thereby forms one double bond to the surface. The middle C-atom does not bind to

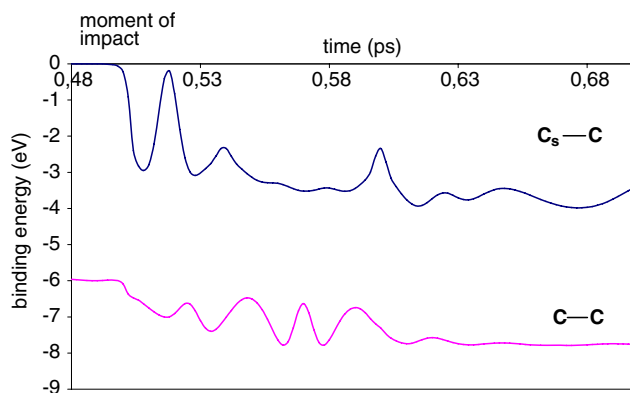


Fig. 3. Evolution of the binding energy between a surface atom and an impinging C_2 radical, and the change from a double C–C bond in C_2 before the impact (~ 6 eV) to a triple C–C bond after the impact (~ 7.8 eV).

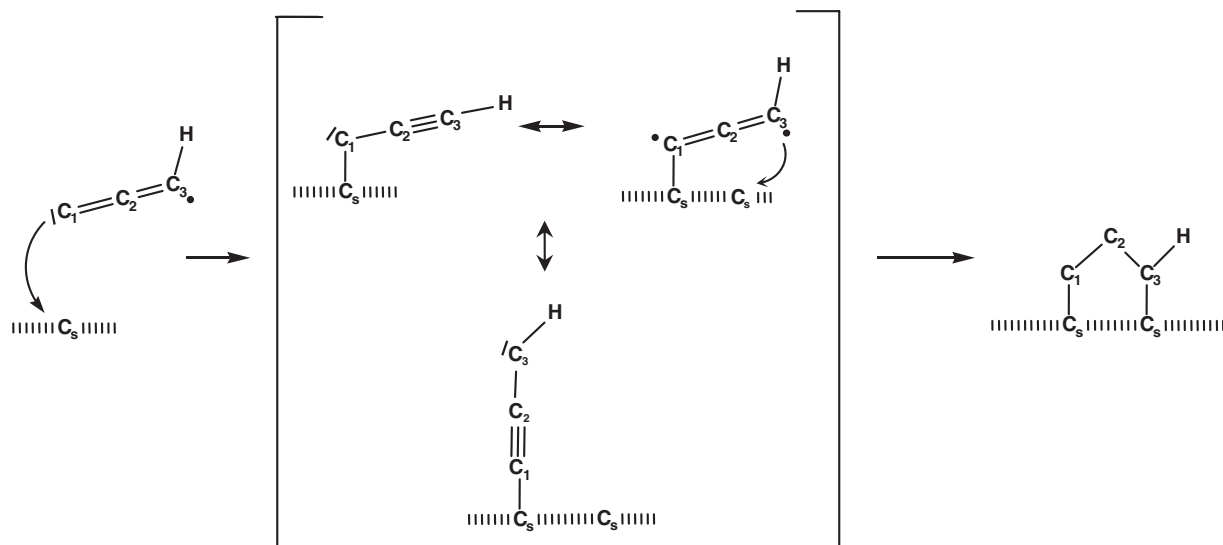


Fig. 4. Bridge formation upon impact and sticking of a *l*-C₃H radical.

the surface, as mentioned above, due to repulsive forces between this atom and the surface. Again, the bond between the middle C-atom and the surface binding atom becomes slightly stronger upon sticking (+1.4%), while the other C–C bond in the radical becomes slightly weaker (–1.3%).

3.2.3. Impact of *l*-C₃H

The sticking coefficient of *l*-C₃H is calculated to be 0.65 on the O4 site, and 0.84 on the O5 site. The lower value on the O4 site compared to the O5 site is again due to steric hindrance. Moreover, the values are slightly lower than for C₃, due to the slightly larger radical, yielding a bit more steric hindrance.

In this case, two sticking mechanisms are possible: the radical binds to the surface either with the outer C-atom, not carrying the H-atom (55% on O4, 46% on O5), or it sticks to the surface with the H-carrying C-atom (10% on O4, 38% on O5). The first mechanism occurs more often than the second one, since the H-atom is shielding the C-atom from the surface. This is especially true on the O4 site. On the O5 site, this effect is diminished due to the fact that the surface atom on the O5 site is not partially shielded by other surface atoms, as is the case on the O4 site. Again, the middle C-atom cannot bind due to repulsive forces.

3.2.4. Impact of *c*-C₃H

It is seen in Table 4 that the *c*-C₃H radicals are again more reactive at the surface than the *l*-C₃H radicals, as the calculated reflection coefficients on sites O4 and O5 are much lower. On site O4, only 4% of the *c*-C₃H radicals are reflected. Simple reflection of the *c*-C₃H radical occurred only in 1% on site O4. In 3% of the cases, it also reflects, but at the same time it abstracts the surface atom from the surface, thereby creating a C₄H species, which then moves away from the surface. In 37% of the impacts, only one of the C-atoms of the radical sticks to the surface, while the remaining H-atom and the two other C-atoms do not stick and are reflected back into the plasma. In another 8% of the impacts, a CH fragment sticks, while the other two carbon atoms reflect. In all other cases (51% of the impacts), the whole molecule sticks to the surface. In all cases investigated, one or several bonds of the *c*-C₃H radical break upon sticking on site O4. Hence, the radical never stays intact upon sticking to the surface.

On site O5, reflection does not occur at all. While on the O4 site, partial sticking occurs regularly (45% of the impacts), this appears not to happen on the O5 site. Also the fraction of impact events causing the break up of the radical decreases to 83%, thereby leaving an intact *c*-C₃H radical stick to the surface in 17% of the cases. In this case, *c*-C₃H sticks to the site with the

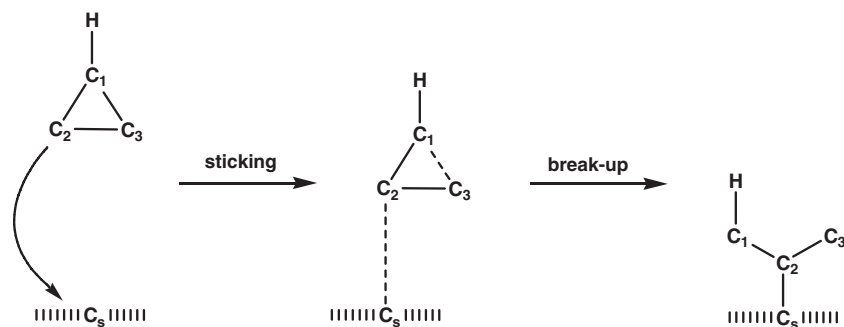


Fig. 5. Schematic representation of the sticking and break-up mechanism of the *c*-C₃H radical, leaving the surface binding atom 3-coordinated.

Table 4
Calculated sticking and reflection coefficients, and sticking structures on sites O4 and O5

Radical	Reflection	Sticking-structures	Sticking	Radical	Reflection	Sticking-structures	Sticking
C_2	O4 : 0.05 O5 : 0.0		O4 : 0.91 O5 : 1.0	$c\text{-}C_3H$ continued			O4 : 0.06 O5 : 0.12
$C-C$			O4 : 0.04 O5 : 0.0				O4 : 0.28 O5 : 0.32
C_3	O4 : 0.23 O5 : 0.09		O4 : 0.77 O5 : 0.91				O4 : 0.13 O5 : 0.33
$C_2\text{-}C_1\text{-}C_3$							
$l\text{-}C_3H$	O4 : 0.35 O5 : 0.16		O4 : 0.55 O5 : 0.46				O4 : 0.0 O5 : 0.17
			O4 : 0.10 O5 : 0.38				O4 : 0.01 O5 : 0.06
$c\text{-}C_3H$	O4 : 0.04 O5 : 0.0		O4 : 0.37 O5 : 0.0				O4 : 0.02 O5 : 0.0
			O4 : 0.08 O5 : 0.0				O4 : 0.01 O5 : 0.0

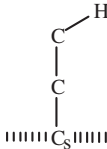
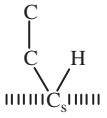
carbon atom carrying the H-atom. This creates a 4-coordinated C-atom, while all the other mechanisms create either a 2-coordinated C-atom (65%), or a 3-coordinated C-atom (18%).

3.3. Site O6

The O6 site consists of a linear C_2H fragment at the surface. On this surface, only the C_2 radical seems to be reactive. The results are summarised in Table 5. C_2 reflects in 66% of its

impacts. In 65% of these reflection events, the C_2 abstracts the H from the surface, and desorbs back into the plasma as a C_2H species. In the remaining 35% of the reflection events, it simply reflects. In only 7% of its impacts, it sticks directly on the upper C-atom of the site. In 27% of its impacts, however, the C_2 radical is ‘inserted’ between the upper C-atom of the site, and the H-atom attached to it. This is a 2-step process: first, one of the C_2 C-atoms abstracts the H from the site. Then, the other C-atom of the C_2 radical (which has by then become a C_2H

Table 5
Calculated sticking and reflection coefficients, and sticking structures on site O6

Radical	Reflection	Sticking-structures	Sticking
C_2	0.66		0.27
C–C			0.07
C_3 , $l-C_3H$ and $c-C_3H$	100%	100% reflection	

radical), binds to the C-atom of the site that was previously carrying the H-atom. In this way, the C_2 radical has inserted itself in the site.

All the other radicals seem to give 100% simple reflection, due to the H-passivation (cfr. site O3).

3.4. Sites O7 and O8

The O7 and O8 sites are identical. However, the position at which the radicals impinge on the site is different: on the O7 site, the middle C-atom is bombarded, while on the O8 site, the radical attacks one of the outer C-atoms. The results are summarised in Table 6.

3.4.1. Impact of C_2

Again, the C_2 radical is very reactive: it has a sticking coefficient of 1.0 on site O7 and 0.98 on site O8. The sticking energy is about -5.1 eV, which is lower than on the O4 and O5 sites, due to the fact that here, the C_s atom becomes 3-coordinated, so that a true double bond cannot be formed. Indeed, all three bonds to the C_s atom become more or less equal in strength. When impacting on site O8, a bridge structure can be formed, although this was found to occur in only 3% of the impacts.

3.4.2. Impact of C_3 and $l-C_3H$

The C_3 radical is not very reactive on these sites, especially on the O7 site, where 95% of its impacts result in reflection, yielding a sticking coefficient of 0.05. On the O8 site, the sticking coefficient increases to 0.22. The only mechanism observed, consists of the C_3 radical sticking with one of its outer C-atoms to one of the site atoms.

The same is true for the $l-C_3H$ radical. It has a sticking coefficient of 0.12 and 0.21 on site O7 and O8, respectively.

Again, it only sticks with one C-atom to one of the site atoms. In this case, the sticking atom is invariably the outer C-atom that is not connected to the H-atom.

3.4.3. Impact of $c-C_3H$

Again, the $c-C_3H$ radical shows the most complex reaction behaviour. Its sticking coefficient is calculated to be 0.29 and 0.59 on site O7 and O8, respectively. While the position of impact on the O8 site is one of the outer C-atoms of the site, the $c-C_3H$ radical can also stick on the middle C-atom in this case. The opposite seems not to occur. The higher sticking coefficient on site O8 than on site O7, can be explained by considering the connectivity of the surface atoms. On site O7, the surface atom under attack is the middle carbon atom. Since this atom is fully bound, the incoming radical will experience repulsive forces from this atom, effectively decreasing the reactivity on this site. On site O8, however, the surface atom under attack is one of the atoms at the site, having a dangling bond, effectively enhancing the reactivity on this site.

On the O8 site, two reaction mechanisms seem to be preferred: in 29% of its impacts, the radical sticks to the outer C-atom of the site, with one of the C-atoms not connected to the H-atom, and without breaking up. In 10% of its impacts, the same mechanism occurs, but now with breaking of the bond between the sticking C-atom and the C-atom that carries the H-atom. Further, it should be noted that in 26% of the impacts on O8, the radical breaks up, and on site O7 this happens in 23% of the impacts.

3.5. Site O9

The O9 site is identical to the O7 site, except for the H-atom connected to one of the outer C-atoms of the site. The mechanisms occurring on this site, are identical to the ones on the O7 and O8 sites. Although the radicals now only impinge on the middle C-atom, some of them also bind to the C-atom at the side (i.e., the one which is not bound to the H-atom). The H-atom serves two functions in this respect: first, it shields the C-atom to which it is connected. Second, it also pushes impinging radicals to the other side of the site, due to repulsion between the H-atom and the impinging radical. The results are summarised in Table 7.

3.5.1. Impact of C_2

The C_2 radical appears to have a sticking coefficient of 1 on this site, and it sticks either on the middle (spotted) C-atom (84% of the impacts), or on the side C-atom which does not carry the H-atom (14%). In the remaining 2 impacts, a bridge structure was formed, in which the radicals sticks with both atoms to both the available site atoms (i.e., not the H-carrying C-atom).

3.5.2. Impact of C_3 and $l-C_3H$

Entirely corresponding to the trend seen on the previous sites, the C_3 and $l-C_3H$ radicals show a much lower sticking coefficient: 0.26 and 0.22, respectively. Again, they bind to the surface with the outer C-atom. The C_3 radical binds mostly on the middle C-atom (23% of its impacts), while the $l-C_3H$ binds in about equal amounts on both the middle and the outer, non-

Table 6
Calculated sticking and reflection coefficients, and sticking structures on sites O7 and O8

Radical	Reflection	Sticking-structures	Sticking	Radical	Reflection	Sticking-structures	Sticking
C ₂	O7 : 0.0 O8 : 0.02		O7 : 1.0 O8 : 0.95	<i>c</i> -C ₃ H continued			O7 : 0.08 O8 : 0.08
C-C							
			O7 : 0.0 O8 : 0.03				O7 : 0.0 O8 : 0.10
C ₃	O7 : 0.95 O8 : 0.78		O7 : 0.05 O8 : 0.22	<i>c</i> -C ₃ H			O7 : 0.07 O8 : 0.04
C ₂ -C ₁ -C ₃							
<i>l</i> -C ₃ H	O7 : 0.88 O8 : 0.79		O7 : 0.12 O8 : 0.21				O7 : 0.0 O8 : 0.02
<i>c</i> -C ₃ H	O7 : 0.71 O8 : 0.41		O7 : 0.06 O8 : 0.04				O7 : 0.08 O8 : 0.02
			O7 : 0.0 O8 : 0.29				

H-carrying C-atom of the site. This is caused by the H-atom of the radical: it interacts with the site atoms, resulting in a ‘push-effect’. The radical is effectively pushed towards the side atom of the site.

The H-atom on the site itself also effectuates a push-effect. However, although the C₃ radical is pushed towards the side, it can still bind to the middle carbon atom more easily, due to the size of the molecule (it has 2 available C-atoms, at both sides), and due to the fact that the C-atom in the middle of the site is sterically more easily available.

3.5.3. Impact of *c*-C₃H

The difference in reactivity between the cyclic and the linear isomer of the C₃H radical is again clearly visible. The *c*-C₃H radical is reflected in only 18% of its impacts, to be compared with 78% of the *l*-C₃H impacts on this site.

The same structures arise as on the previous two sites. In 38% of the impacts, the radical stays intact, and then it sticks a bit more easily at the side of the site (22% vs. 16% on the middle C-atom). If a bond is broken during the sticking event, then the radical will stick more easily on the middle atom of the site. In

Table 7
Calculated sticking and reflection coefficients, and sticking structures on site O9

Radical	Reflection	Sticking-structures	Sticking	Radical	Reflection	Sticking-structures	Sticking
C_2	0.0		0.84	<i>l</i> - C_3H continued			0.10
$C-C$				<i>c</i> - C_3H	0.18		0.22
			0.14				
			0.02				0.16
C_3	0.74		0.23				
$C_2-C_1-C_3$							
			0.03				0.14
<i>l</i> - C_3H	0.78		0.12				0.05
				<i>c</i> - C_3H continued			0.07
							0.03

only 5% of all impacts, the radical will break up and stick on the available C-atom at the side.

3.6. Sites O10 and O11

The last two sites we have simulated are a variation on the three previous sites. On both the outer carbon atoms of the site,

a H is attached. Again, the radicals can impinge on both the middle carbon atom, and on one of the side carbon atoms. The results are summarised in Table 8.

3.6.1. Impact of C_2

As is already clear from the above, the C_2 radical is very reactive, and its reaction behaviour leads to structures not found

Table 8
Calculated sticking and reflection coefficients, and sticking structures on sites O10 and O11

Radical	Reflection	Sticking-structures	Sticking	Radical	Reflection	Sticking-structures	Sticking		
C_2	O10 : 0.0 O11 : 0.05		O10 : 1.0 O11 : 0.72	$c-C_3H$	O10 : 0.03 O11 : 0.17		O10 : 0.38 O11 : 0.33		
$C-C$			O10 : 0.0 O11 : 0.16				O10 : 0.21 O11 : 0.29		
			O10 : 0.0 O11 : 0.07				O10 : 0.21 O11 : 0.03		
C_3	O10 : 0.48 O11 : 0.42		O10 : 0.52 O11 : 0.58	$C_2-C_1-C_3$			O10 : 0.14 O11 : 0.12		
$l-C_3H$	O10 : 0.69 O11 : 0.65		O10 : 0.31 O11 : 0.29				O10 : 0.03 O11 : 0.06		
			O10 : 0.0 O11 : 0.06						

for the other radicals, as will be shown below. The other radicals only stick on the middle carbon atom of the site (if they stick), but the C_2 radical can also stick on the outer C-atoms.

On the O10 site, the impact position of the radical is the middle C-atom of the site. The sticking coefficient of the C_2 radical is then calculated as 1.0. In all cases, the mechanism is straightforward: the C_2 radical simply sticks with one of its atoms on the middle C-atom of the site, with the formation of a medium strong bond of (on average) -4.88 eV. Recall that the average single C–C bond strength is about -3.60 eV, a double bond about -6.36 eV, and a triple bond about -8.70 eV. The C–C bond in the C_2 radical is weakened by about 3% compared to the gas phase.

On the O11 site, however, the impact position is one of the side atoms. The sticking coefficient remains very high (0.95), and most sticking events yield the same structure as sticking on O10: the C_2 radical being bound to the central C-atom of the site (72% of its impacts). In 16% of its impacts, the radical also binds to the middle carbon atom, but the H-atom from the side has shifted from the side-atom to the upper C_2 -atom. In the remaining 7% of its impacts, the C_2 radical sticks on the side atom. The H-atom is replaced by the C_2 -radical, and becomes bound to the upper atom of the C_2 fragment, as was also the case on site O6. In the events where the H-atom becomes bound to the C_2 -radical, this H-shift stabilizes the C–C bond, and strengthens the bond between the site-atom and the radical, as compared to sticking on the O10 site. This can be explained by the fact that removal of the H-atom induces several resonance structures, donating electrons to the C_s – C_2 bond and the C_2 fragment.

3.6.2. Impact of C_3

The C_3 radical has a calculated sticking coefficient of 0.52 and 0.58 on site O10 and O11, respectively. Only one structure it formed: one of the outer C-atoms becomes connected to the middle carbon atom of the site. Again, the C–C bond connecting the surface binding atom of the radical and the middle carbon atom of the radical becomes slightly stronger (about 1.5%), while the other bond of the radical becomes slightly weaker by about 1.2% and 1.7% on both sites, respectively.

Remarkable however is the fact that the presence of H on the sites seems to enhance the sticking of this radical: the sticking coefficient of C_3 increases from 0.05 on site O7, to 0.26 on site O9, and to 0.52 on site O10 (same impact position).

3.6.3. Impact of l - C_3H

The stabilizing effect of the H-atom(s) on the site is also visible for the l - C_3H radical, although to a lesser extent. In the series of impacts on sites O7, O9 and O10, its calculated sticking coefficient goes up from 0.12 to 0.22 to 0.31.

On the O10 site, the l - C_3H radical only sticks through its outer available non-H-carrying carbon atom, binding to the middle carbon atom of the site. On the O11 site, the sticking coefficient is calculated to be 0.35. In this case, 83% of its sticking events (or 29% of the impacts) occurs through the same mechanism as on the O10 site, whereas in the remaining events, the carbon atom carrying the H-atom of the radical, sticks to the

middle carbon atom of the site. In this case, the C–C bond connecting the carbon atom of the radical that binds to the site, and the middle carbon atom of the radical, is weakened strongly by almost 20%.

3.6.4. Impact of c - C_3H

The c - C_3H radical is very reactive on the O10 site, showing a sticking coefficient of 0.97. In 38% of its impacts, the bond between the sticking atom and the H-carrying C-atom of the radical is broken. The surface sticking atom is one of the ‘available’ radical carbon atoms. In this case, the surface sticking atom becomes 2-coordinated. In 21% of the impacts, the radical simply sticks, without the breaking of a bond. Now, the surface sticking atom becomes 3-coordinated. Two other mechanisms also leave the surface sticking atom 3-coordinated: in 21% of the sticking events, the bond between the H-carrying atom, and the carbon atom that is not bound to the surface breaks. The third carbon atom then binds to the surface. In a few cases (3% of the impacts), the H-carrying atom itself binds to the surface. The bond connecting this atom and one of the two other carbon atoms then breaks. Finally, one last mechanism is observed, in which the bond between the two carbon atoms that do not carry the H-atom breaks. The radical then sticks with one of these atoms (14% of the impacts).

On the O11 site, the same reactions are observed. However, the sticking coefficient is now lower, with a calculated value of 0.83.

4. Conclusion

Molecular dynamics studies using the Brenner potential have been carried out to investigate the sticking behaviour of several radicals typically observed in the expanding thermal plasma. Specific sites have been built, to gain insight in the deposition mechanism of thin a-C:H films. The radicals studied here include C_2 , C_3 , l - C_3H and c - C_3H .

It is observed that C_2 is the most reactive of these species, and capable of H-abstraction from the surface.

The C_3 radical shows a moderate sticking coefficient of on average about 0.5. The middle carbon atom never binds to the surface due to repulsive forces induced by the fully bound central atom. The two other carbon atoms, however, are available and reactive, and hence, bridge structures are easily formed.

Comparing the two C_3H isomers, it is clear that the cyclic variant is much more reactive, having a sticking coefficient of on average 0.73. The linear radical on the other hand is less reactive, with a sticking coefficient of about 0.42. This can be explained by the fact that (1) the cyclic radical easily breaks up, enhancing its reactivity; (2) the central carbon atom in the linear isomer is fully bound, inducing repulsive forces with the substrate (identical to C_3), leaving only the outer C-atoms available and reactive, whereas the cyclic variant does not have such a fully bound C-atom; and (3) the H-atom in the linear isomer shields one of the two outer carbons, leaving only one of the atoms available and reactive. Hence, the least reactive species is the linear C_3H radical.

These results are important for the study of the expanding thermal plasma, in which these species have been observed [7]. They allow us to gain insight into how the a-C:H films, grown with this source are actually deposited. Second, these results are also relevant for film growth in general. For instance, it is clearly shown that sticking coefficients of hydrocarbons on a-C:H surfaces are site dependent. It is likely that this is also true on other covalently bound materials. Finally, these results are also important as input for plasma simulations, where knowledge of sticking coefficients is of great importance.

Acknowledgments

E. Neyts is indebted to the Institute for the Promotion of Innovation by Science and Technology in Flanders (IWT-Flanders) for financial support. The authors would like to thank J. Benedikt and M.C.M. van de Sanden for the many fruitful discussions on the chemistry in the ETP plasma and the deposition mechanisms, and also Prof. R. Gijbels for the interesting discussions.

References

- [1] S. Aisenberg, R. Chabot, *J. Appl. Phys.* 42 (1971) 2953.
- [2] J. Robertson, *Mater. Sci. Eng.* R37 (2002) 129.
- [3] J. Robertson, *J. Non-Cryst. Solids* 299–302 (2002) 798.
- [4] <http://www.bekaert.com/bac/Products/Diamond-Like%20Coatings.htm>.
- [5] P. Koidl, C. Wagner, B. Dischler, J. Wagner, M. Ramsteiner, *Mater. Sci. Forum* 52 (1990) 41.
- [6] J. Benedikt, M. Wisse, R.V. Woen, R. Engeln, M.C.M. van de Sanden, *J. Appl. Phys.* 94 (2003) 6932.
- [7] M. Meier, A. von Keudell, *J. Appl. Phys.* 90 (2001) 3585.
- [8] J. Benedikt, D.J. Eijkman, W. Vandamme, S. Agarwal, M.C.M. van de Sanden, *Chem. Phys. Lett.* 402 (2005) 37.
- [9] V.V. Serikov, S. Kawamoto, C.F. Abrams, D.B. Graves, *APS Proceedings of the "22nd Symposium on Rarefied Gas Dynamics"*, Sydney, 2000.
- [10] D.W. Brenner, *Phys. Rev.*, B 42 (1990) 9458.
- [11] W.C. Swope, H.C. Anderson, P.H. Berens, K.R. Wilson, *J. Chem. Phys.* 76 (1982) 637.
- [12] H.J.C. Berendsen, J.P.M. Postma, W.F. van Gunsteren, A. DiNola, J.R. Haak, *J. Chem. Phys.* 81 (1984) 3684.
- [13] D.N. Ruzic, et al., *Presentation at the 10th International Workshop on Carbon Materials for Fusion Application*, Jülich, Germany, 17–19 September, 2003.